IMPROVED HYDROGENERATOR FIELD WINDING THERMAL MONITORING

by

Ilija G. KLASNIĆ[a,b*], Jasna D. DRAGOSAVAC[b], and Zoran M. LAZAREVIĆ[a]

[a] School of Electrical Engineering, University of Belgrade, Belgrade, Serbia
[b] Electrical Engineering Institute Nikola Tesla Belgrade, University of Belgrade, Belgrade, Serbia

Original scientific paper
https://doi.org/10.2298/TSCI221212036K

A new monitoring method for determination of average hydrogenerator field winding temperature is introduced in order to increase the robustness of the temperature measurement system using the classic U-I method. The classic approach is prone to error due to brush voltage drop, especially when field voltage is low. Developed thermal model is based on field current and cold cooling air temperature measurements, as well on temperatures acquired from digital temperature sensors mounted across the field winding. To monitor the rotor temperature for generators with brushless excitation where field voltage and current measurements are not accessible, a mathematical model was developed to estimate the average field winding temperature based on the existing temperature monitoring of the cooling medium and mounted sensors. Importance of the proposed approach arises from the foreseen widespread use of brushless generators in distributed generation. The developed models were compared and their sensitivity was examined thoroughly.

Key words*: temperature estimation models, temperature measurement method, wireless temperature measurements, average field winding temperature*

Introduction

In a high performance power system with high RES penetration, overheating of the synchronous generator (SG) is an important limiting factor for supporting system stability. Stability system services are one of the key to unlocking renewable power's full potential. The SG are the main grid elements to cope with the transients. With high RES penetration, it is possible to have a large number of underloaded SG to provide flexibility. The question is whether there is any additional capability above rated on SG that can be activated and used in a few tens or hundreds of seconds after a disturbance occurs without endangering the generator itself. The working area of the SG is presented in fig. 1 and is limited by thermal conditions according to Boundaries I (stator windings thermal limit) and Boundaries II (field winding thermal limit). Regarding temperatures, SG are rated up to their winding insulation class, *e.g.* 155 °C for Class F, before irreversible damage or reliability issues can occur, Curve 2 in fig. 2(a) [1].

To keep the SG below that limit, the performance is throttled by limiting the windings current at a safe level defined by Curve 1 in fig. 2(a) [2]. This safe level includes safety margins up to the maximum allowed temperature because of unknown hotspot temperature, fig. 2(b). As shown in fig. 2(b), temperature accuracy directly influences the amount of safety margin

* Corresponding author, e-mail: ilija.klasnic@ieent.org

that needs to be built-in into the temperature measuring system. To account for this error, the capability of the SG needs to be reduced. Also, in [1, 2] it is assumed that the SG is overloaded starting from temperatures corresponding to rated operating point, fig. 2(a), where Curve 1 represents the setting of the field current limiter and Curve 2 thermal damage curve of typical SG. In both cases, the winding was at operational temperature for rated conditions before overloading.

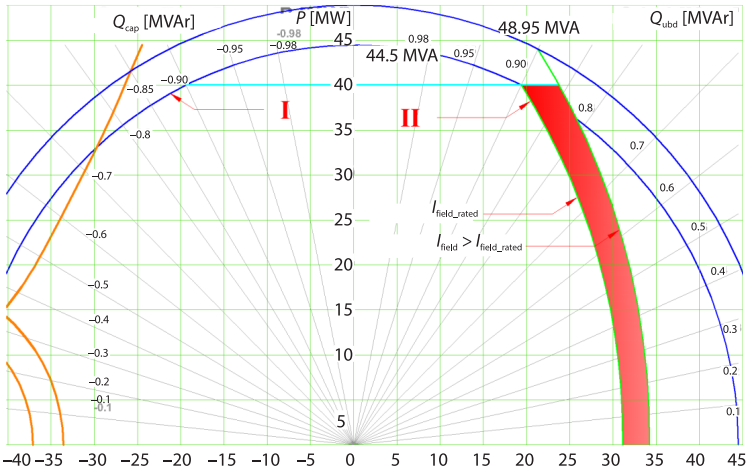

Figure 1. Capability P-Q diagram of SG with its limits and temporary overload zone

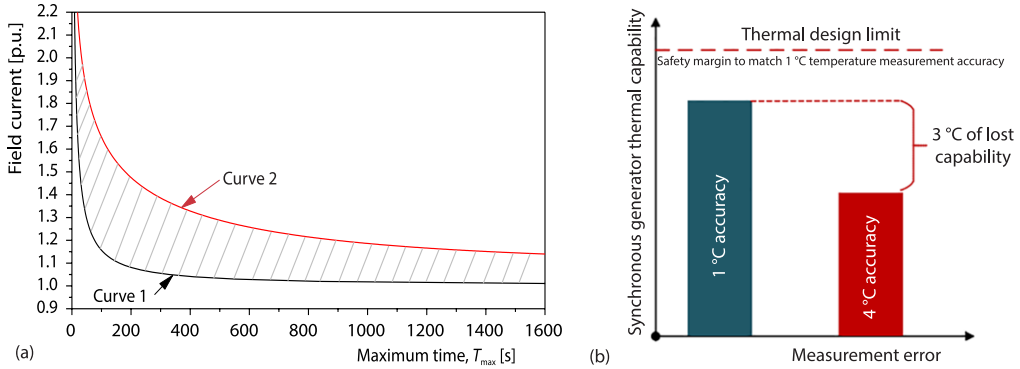

Figure 2. (a) Curve 1 is overexcitation limiter setting of standard SG for supporting system by overloading field winding, Curve 2 is a thermal damage curve of typical SG, in both cases the winding was at operational temperature (*e.g.* t = 95 °C) for rated conditions before overloading and (b) capability margins due to temperature measurement inaccuracy

Therefore, there is a need for accurate rotor temperature estimation because if a transient in the power system occurs when the temperature of the SG is under the rated operating point, the generator overload may last a few seconds longer, which can sometimes be a decisive factor in preventing collapse. A small variable capability (overload zone) can be defined outside the area allowed by the P-Q diagram, whose boundaries vary with the generator temperatures and the magnitude of the field overcurrent. Unfortunately, getting accurate and quick temperature measurements of the field (rotor) winding can be challenging. Unlike the stator, the rotor

of the SG is not equipped with temperature sensors built into the SG during construction even though the thermal stress is one of the most important causes of rotor winding failure. In Hudon *et al.* [3], it is showed that in 27.3% of hydrogenerators, the rotor is more thermally stressed than the stator, while in another 27.3% the rotor and the stator are under the same thermal stress.

Many authors are trying to improve rotor temperature monitoring systems by introducing modern direct temperature measurement technologies. In Hudon *et al.* [4], the installation of Fiber Bragg Gratings on a 74.75 MVA generator is presented, along with temperature readings at 60 locations. These temperatures are compared to the average field winding temperature, determined by the standard voltage-current (*U-I*) method. In Hudon *et al.* [3], the characterization of an IR thermal sensor installed on the stator side to measure the rotor temperatures is presented. The probe is inserted through a vent duct of the stator all the way to the air gap where it measures the temperature of the pole passing at a tangential speed in the range of 200 km/h roughly 15 mm from the probe tip. It improves the thermal diagnosis of rotor poles and represents the basis for understanding all the factors influencing the losses and cooling of rotor poles. Measurements in [3, 4] are related to large-scale hydrogenerators in real power plant implementations. In Mori *et al.* [5], correlation is established between CFD calculations and laboratory measurements using IR camera. However, the obtained results showed the necessity of combining measurements with calculations in order to achieve a good thermal rotor representative. In Pelle and Souad [6], a new cooling solution of 750 kW wind generator is investigated. The influence of a jet on the convective heat transfers on a rotor surface is investigated through measurements and calculations. It has been shown that the measurements can be valuable for determining the actual heat distribution across a discoidal rotor surface. In Kral *et al.* [7], in order to provide a reference for the obtained rotor temperature estimation technique, an IR sensor was mounted inside the 210 kW induction motor. The measured rotor temperature represents the temperature of the end ring at the driving end (opposite side of the cooling fan). This measured temperature does not match the estimated rotor temperature exactly, since the estimated temperature is composed of the rotor end ring and the rotor bar temperature. The methods proposed in [5, 7] use expensive high speed IR cameras to get 2-D temperature field images of visible rotor surfaces at laboratory size machines. In Stipetic *et al.* [8], an industrial IR thermometer, which represents an alternative to expensive fast IR thermometers or cameras, is used for the determination of the dynamic limit in the P-Q diagram of a SG due to excitation winding overheating. The effect of the interpolar surface can be cancelled if the IR thermometer is positioned at a certain angle with respect to the machine's main axis. Digital temperature sensors have been mounted on the rotor to measure the excitation winding surface temperature for comparison. It has been shown that the IR elements' mounting location and specifics can be essential for obtaining accurate measurements. In Kovačić *et al.* [9], a prototype of digital wireless measurement system using 1-wire temperature sensors and a Bluetooth transceiver has been developed and mounted on a 400 kVA, 1000 rpm SG. The aim of the paper was to determine the dynamic limit of the generator due to excitation winding overheating. Authors suggested combining calculation of temperature distribution on the excitation winding using the FEM model and temperature sensor values as inputs.

In the presented literature overview, the effectiveness of the proposed direct temperature measurements is verified by comparison with the standard indirect method. Indirect method is based on field current and voltage measurements and highly depends on the accuracy of these measurements, especially field voltage measurement. In contrast to indirect method that is represented in the standards and practice, the direct methods are significantly less widely used. Direct methods require installation of additional temperature sensors on:

– rotating rotor which is related with several potential problems: location of the mounted temperature sensor, complex data transmission, harsh environment *etc*., or
– stator whereby the temperature of the surface that is rotating in front of the sensor at the observed moment is measured.

Ideally, the temperature sensor should be placed as close to the field winding as possible and away from other heat sources including coolant flow, in order to get accurate temperature measurement. The main feature of the direct method is that provides information about the local temperature of a part of the field winding on which the temperature sensor is mounted, unlike the indirect one which provides only an average field winding temperature. Both methods show significant shortcomings when used individually on site that can be compensated by their combined use. Therefore, a physical thermal model that links the results of various reliable measurement methods is necessary.

In this paper two average field winding temperature estimation models are developed based on: direct temperature measurements installed on the rotor of 44.5 MVA hydrogenator (HG), standard cold air temperature measurements combined with field current measurements, when available. Less accurate field voltage measurement is omitted. The aim of the developed estimation models is to increase the accuracy, reliability and robustness of the field winding temperature monitoring system. The estimation models coefficients are determined using experimental data, collected from the heat run test performed on 44.5 MVA HG, as inputs. Calculated average field winding temperatures using developed models are verified by comparing with temperatures obtained by on-site measurements with a modified indirect method of increased accuracy.

Field winding temperature estimation models

Proposed models rely on temperature readings from digital embedded temperature sensors installed as a part of wireless rotor temperature monitoring system and standard measurements such as field current and cold air temperature. The models are valid in the stationary state as the worst case scenario. During the transient process, the field winding temperature is lower and reaches its maximum in the thermal steady-state. The feature of the field current measurement, in contrast with field voltage measurement, is that it is less contaminated by electromagnetic noise because of the high inductance of the field winding. The cold air temperature is accurately measured and the cooling air itself represents a system of low thermal capacity and therefore, reacts quickly to changes. In order to develop a multipurpose model that could also be used with brushless generators that do not have field current measurement available, the first model relies only on direct temperature measurements and cold air temperature measurements, which are always available. In the second model, the accuracy of the estimator is increased by including the field (excitation) current value.

Estimator based on direct field winding and cold air temperature measurements (Model 1)

Air cooled HG rotor pole, shown in fig. 3(a), can be modelled as a simplified reduced heat exchanger given in fig. 3(b), where $t_{\text{cold,air}}$ is the cold air or inlet temperature, $t_{\text{rot.outlet,air}}$ is the rotor hot air or outlet temperature and $t_{\text{rot.avg}}$ is the average temperature of the field winding determined by the indirect voltmeter-ammeter resistance method. Dissipated heat is directed from solid copper slab, representing rotor pole winding, to the cooling air. In reality, the cooling air temperature would follow an exponential rise, but in this analysis the linear rise approximation is assumed. The proof of made assumption is indirect. Good agreement between measured and

estimated temperature values using the aforementioned assumption in the thermal steady-state is achieved. In such a way the equivalent thermal network shown in fig. 4(a) can model the thermal process where thermal resistance R_{th1} is a constant value.

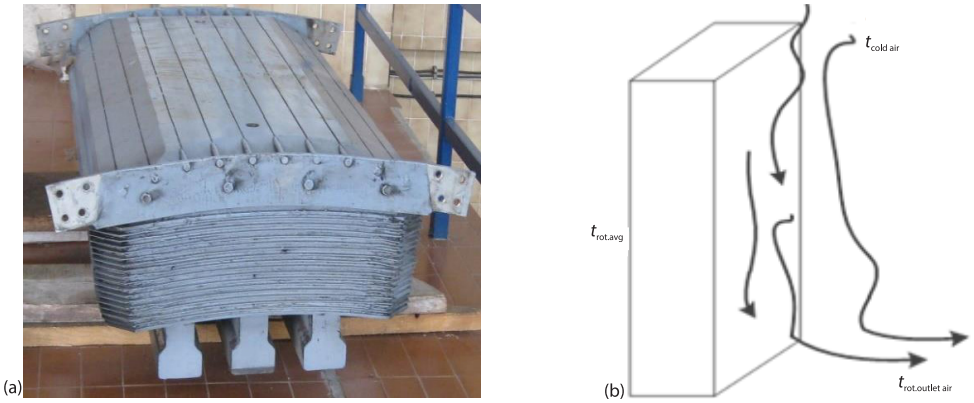

Figure 3. (a) HG rotor pole and (b) simplified model of rotor pole cooled by air-flow

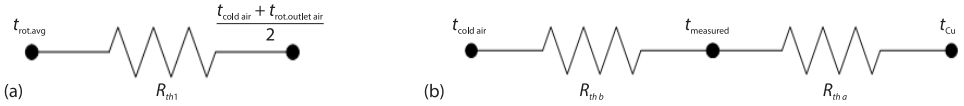

Figure 4. (a) Equivalent thermal network representing heat flow in heat exchanger shown in fig. 3(b) and equivalent thermal network representing mounted temperature sensors for field winding temperature measurement

During the cooling process of the field winding, the cooling air temperature is increasing and the rotor outlet air temperature $t_{rot.outlet,air}$ can be given:

$$t_{rot.outlet,air} = t_{cold,air} + \frac{R_f I_f^2}{q \rho_{air} c_{air}} \tag{1}$$

where R_f is the field winding resistance and I_f – the field current. The second term on the right-hand side of eq. (1) represents the cooling air temperature rise due to Joule losses in the field winding. According to fig. 4(a) the heat flow equation describing steady-state of the field winding cooling process can be written by using the analogy between electrical quantities and temperatures:

$$R_f I_f^2 R_{th1} = t_{rot.avg} - \frac{1}{2}\left(t_{cold,air} + t_{cold,air} + \frac{R_f I_f^2}{q \rho_{air} c_{air}} \right) \tag{2}$$

By rearranging eq. (2) the equation is derived:

$$t_{rot.avg} = t_{cold,air} + C_1 I_f^2 \tag{3}$$

where C_1 is a constant coefficient. Equation (3) enables determination of the average field winding temperature via cold air temperature and square of the field current. The importance of eq. (3) is that rotor outlet hot air temperature, which is not part of the standard set of measurements in HG, unlike cold air temperature and field current, can be omitted.

Temperature sensors are influenced by the stream of the cold cooling air since they are placed close to the air inlet into the inter-pole space. According to the equivalent thermal

network shown in fig. 4(b), the temperature sensor readings are the temperatures at the middle point of the thermal resistance divider, so the sensor temperature readings t_{measured} can be expressed:

$$t_{\text{measured}} = \frac{t_{\text{cold air}} R_{\text{th a}} + t_{\text{Cu}} R_{\text{th b}}}{R_{\text{th a}} + R_{\text{th b}}} = a t_{\text{col ,air}} + b t_{\text{Cu}} \tag{4}$$

where a and b are constant coefficients and t_{Cu} is pole-to-pole connection temperature. The pole-to-pole connection is implemented as copper plate and is heated in two ways: from internal heat generation due to field current flow and also due to heat conducted from the field winding through copper plate cross-section. Having this in mind, the equation can be written:

$$I_{\text{f}}^2 C_2 = t_{\text{Cu}} - t_{\text{cold,air}} \tag{5}$$

where C_2 is a constant coefficient. By combining eqs. (4) and (5) the expression can be derived:

$$t_{\text{measured}} = a t_{\text{cold,air}} + b\left(I_{\text{f}}^2 C_3 + t_{\text{cold,air}} \right) \tag{6}$$

where C_3 is a constant coefficient. Finally, from eqs. (3) and (6) the expression can be derived:

$$t_{\text{rot.avg}} = C_4 t_{\text{measured}} + C_5 t_{\text{cold,air}} \tag{7}$$

where C_4 and C_5 are constant coefficients. Equation (7) is an important relation which enables the mutual comparison of two independent methods for field winding temperature measurement, an indirect $t_{\text{rot.avg,}}$ and the direct one t_{measured}. In addition, comparison is made via cold air temperature, which is part of the standard set of HG measurements. This estimation model can be particularly useful for SG with brushless exciters where field current measurement is not accessible.

Estimator based on direct field winding temperature measurements, field current and cold air temperature measurements (Model 2)

Power dissipated from surface of the pole-to-pole connection P_{diss} can be written:

$$P_{\text{diss}} = C_6 \left(t_{\text{measured}} - t_{\text{cold,air}} \right) \tag{8}$$

where C_6 is a coefficient. On the other hand, the total rate of heat flowing into the pole-to-pole connection is:

$$P_{\text{diss}} = R I_{\text{f}}^2 + \lambda A \left(t_{\text{measured}} - t_{\text{rot.avg}} \right) \tag{9}$$

The first term on the right-hand side of eq. (9) takes into account Joule losses in the pole-to-pole connection and the second one represents heat flow by conduction from the field winding to pole-to-pole connection. From eqs. (8) and (9), the equation can be written:

$$\begin{aligned} t_{\text{rot.avg}} &= \left(1 - \frac{C_7}{\lambda A} \right) t_{\text{measured}} - \frac{r}{\lambda A} I_{\text{f}}^2 + \frac{C_7}{\lambda A} t_{\text{col, air}} \\ t_{\text{rot.avg}} &= C_8 t_{\text{measured}} + C_9 I_{\text{f}}^2 + C_{10} t_{\text{cold,air}} \end{aligned} \tag{10}$$

where C_8, C_9 , and C_{10} are constant coefficients. Equation (10) enables estimation of the average field winding temperature based on mounted temperature sensor readings, field current and cold air temperatures. Equation (10) also enables the mutual comparison of two independent methods for field winding temperature measurement, an indirect and the direct one.

Cross-checking of the results obtained by applying the proposed models was performed with the help of indirect measurements carried out on the real object.

Validation of proposed estimation models through experimental measurements

The accuracy of the average field winding temperature estimator models is confirmed by comparing the calculated results with experimental ones. For this purpose, a heat run test was performed on HG at hydro power plant (HPP) Pirot. In the HPP Pirot, during generator exploitation, pole-to-pole connections have been cracked periodically. The first assumption was that the cause of the problem was local overheating of the pole-to-pole connection. Since the indirect measurement of the field winding temperature provides information only about the average temperature, digital temperature sensors were mounted directly on the pole-to-pole connections with the aim of local temperature real-time monitoring. Details regarding the practical implementation of measurements, as well as difficulties in their application, are presented. All the necessary data about the HG itself and the associated cooling system are provided. Then, the measurement results for six achieved thermal steady-states are given, which are used to evaluate the quality of the developed models. A sensitivity analysis was performed to examine the robustness of the estimation models.

Practical realization of indirect and direct field winding temperature measurements

The HG has a rating of 44.5 MVA, rated voltage 10.5 kV, rated field current 603.5 A and rated frequency 50 Hz. During the heat run test HG was connected to the grid and operated in six regimes. The relevant electrical values and temperatures were simultaneously measured until the thermal steady-state was established. The HG is equipped with a closed air-cooling system with six air coolers spaced symmetrically around the periphery of the stator frame. The cooling air circulation is provided by two axial fans mounted on the bottom and upper side of the rotor. Generated heat from the stator winding and core, and field winding is removed by cooling air and then transferred to the cooling water in the air-to-water heat exchangers.

Indirect voltmeter-ammeter resistance measurement method

Average field winding temperature of HG was indirectly measured using voltmeter-ammeter resistance measurement method [10]. Indirect method is based on precise and simultaneous measurements of field voltage and current. Measuring accuracy highly depends on the accuracy of the field voltage measurement. Diagram of an indirect field winding tempera-

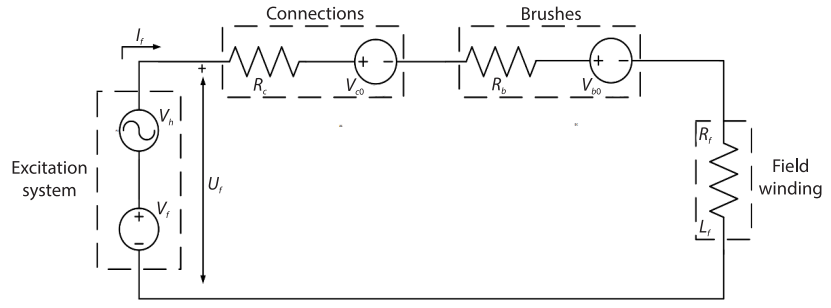

Figure 5. Indirect field winding temperature measurement circuit model using *U-I* method

ture measurement of HG is shown in fig. 5. The field voltage, U_f, contains a large amount of noise, V_h, due to the switching nature of thyristor operation in HG excitation system. The measurement error is a consequence of the voltage drop on the connections between the excitation system and the field winding (V_{c0}, R_c) as well as on the brushes (V_{b0}, R_b) [10-12]. To compensate for these phenomena, it is necessary to measure field voltage with suppressed unwanted electromagnetic noise [10]. This is done through direct copper contact with slip rings with a voltmeter that has an internal resistance in the range of 10-20 kOhm/V, preferably through a suitable low pass filter [11].

The field winding temperature t_f was calculated:

$$t_f = \frac{1}{R_f^{\text{cold}}}\left[k\left(R_f - R_f^{\text{cold}}\right) + R_f t_f^{\text{cold}}\right] \tag{11}$$

where R_f^{cold} is measured field winding resistance at the reference temperature t_f^{cold}, R_f – the measured field winding resistance at temperature t_f, and k – the material coefficient given by the equipment manufacturer (234.5 for pure Cu). Although this method is relatively easy to apply and widely used, it has a drawback that gives only average value of the field winding temperature and can significantly underestimate the rotor hot spot temperature [13].

Direct wireless on-line temperature monitoring system of rotor

The direct field winding temperature measurement method is significantly less widely used, closely related to sensor location, and is still quite expensive. Direct field winding temperature measurement requires installation of temperature sensors on a rotor that rotates at high speed and a complex data transmission device that increases the total cost of the system [14, 15]. Another problem is the harsh environment (large centrifugal force, rotating shaft, *etc.*) in which this system must work reliably. The sensor location, good thermal contact and high thermal insulation from the cooling medium are of utmost importance for the quality of measurement and its usability.

Lay-out of mounted temperature sensors on the first three out of 12 rotor poles in HPP Pirot is shown in fig. 6(a). The first group of sensors, t_1, that are placed on the external pole-to-pole connections, is marked in blue, the second group of sensors, t_3, placed on the leading

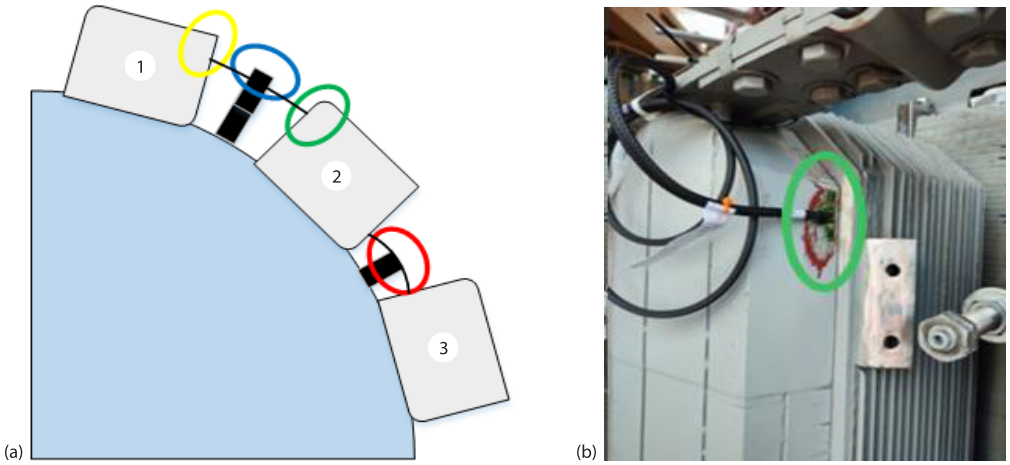

Figure 6. (a) Lay-out of mounted temperature sensors on rotor in HPP Pirot and (b) zoomed-in detail of the mounted temperature sensor on the lagging side of rotor pole

side of pole core is marked in yellow, the third group of sensors, t_4. placed on the lagging side of pole core is marked in green and the fourth group of sensors, t_2, placed on the internal pole-to-pole connections is marked in red. A zoomed-in detail of the temperature sensor placement is shown in fig., 6(b). System comprises the following elements: 48 high precision digital temperature probes DS18S20 with accuracy ±0.5 °C, 232 Vdc-5 Vdc power supply module, rotor processing unit (slave), stator processing unit (master), antenna and data acquisition system for data display and analysis. The system is powered on as soon as the HG is excited. All measured temperatures enter the rotor processing unit from where are wirelessly sent to the stator processing unit located outside the generator pit. The application for data acquisition was developed in National Instruments LabVIEW in which the temperature of each sensor, together with the time base, is logged as a text file which is used for further analysis.

The main disadvantage of the applied system for direct field winding temperature measurement is the large exposure of the pole-to-pole connections to the cooling air-flow. By applying the developed estimation models, the measurement uncertainty of both described measurement methods can be significantly reduced.

Experimental measurements

Heat run test or temperature rise test is one of the type tests of HG. It is performed by choosing the desired generated active and reactive power that makes the winding and core temperature rises. The test is maintained until constant temperature is reached (thermal steady-state). Measured electrical values (I_f is the field current, P, Q are the active and reactive generator power, respectively), temperatures obtained from wireless on-line temperature monitoring system, t_1-t_4, cold air temperature, $t_{\text{cold air}}$, and indirectly measured field winding temperature, t_f, during six operating regimes of the heat run test are collected in tab. 1. Coefficients from eq. (7), Model 1, and eq. (10), Model 2, are determined using the least squares method applied on measured data and shown in tab. 2. The estimated temperature values using Model 1 and Model 2 *vs.* measured average field winding temperature are shown in figs. 7(a) and 7(b), respectively, while error calculated as difference between estimated using Model 1 and Model 2 and measured average field winding temperature are shown in figs. 7(c) and 7(d), respectively. When using field current measurements (Model 2) the achieved temperature estimation accuracy is within ±1 °C, while relying on direct temperature measurements and cold air measurement (Model 1) the average field winding temperature estimation error is higher and is within the range ±6 °C. The estimation accuracy strongly depends on sensor location showing higher accuracy when sensors are mounted as in sensor groups t_2 and t_4 (error is within the range ±2.5 °C), as it is shown in figs. 7(c) and 7(d). The verified estimation models represent a step forward in relation graphical comparison of two experimental measurement approaches given by other authors [4, 8]. In order to check the robustness of the model that does not require field current measurement (in case of brushless generators), the sensitivity of both models was determined.

In previous analyses, the copper resistance with temperature change is neglected, R_f was assumed to be constant. For the range of field currents between 333 A and 604 A and corresponding recorded average field winding temperature rises, the two equations are compared:

$$\Delta t_{\text{rot}} = \frac{AI_{\text{f}}^2 + B}{C - \dfrac{DI_{\text{f}}^2}{235}} \tag{12}$$

$$\Delta t_{rot} = AI_{\text{f}}^2 + B \tag{13}$$

Table 1. Measured temperatures and electrical values during the heat run test

Regime No.	t_1 [°C]	t_2 [°C]	t_3 [°C]	t_4 [°C]	I_f [A]	$t_{cold,air}$ [°C]	P [MW]	Q [MVAr]	t_f [°C]
	Min/Max	Min/Max	Min/Max	Min/Max					
1.	43/44	46/48	38/40	42/44	384.4	23.00	30	0	78
2.	48/49	52/54	42/44	47/50	450.8	24.50	40	0	90
3.	52/54	58/60	45/48	52/57	604.2	25.30	40	19.4	113
4.	47/48	51/54	41/44	47/50	534.8	23.70	30	14.5	97
5.	42/44	46/48	38/39	41/44	333.2	23.10	30	-5.5	76
6.	47/49	51/53	42/43	46/49	412.2	24.50	40	-4.5	86

Table 2. Coefficients of estimation models experimentally determined for sensor groups t_1, t_2, t_3, and t_4

Sensor group	C_4	C_5	C_8	C_9	C_{10}
t_1	5.78	–7.80	1	0.0001024	0.837
t_2	4.08	–5.23	1	0.00009337	0.716
t_3	6.03	–7.10	1	0.0001028	1.042
t_4	3.52	–3.44	1	0.00008879	0.916

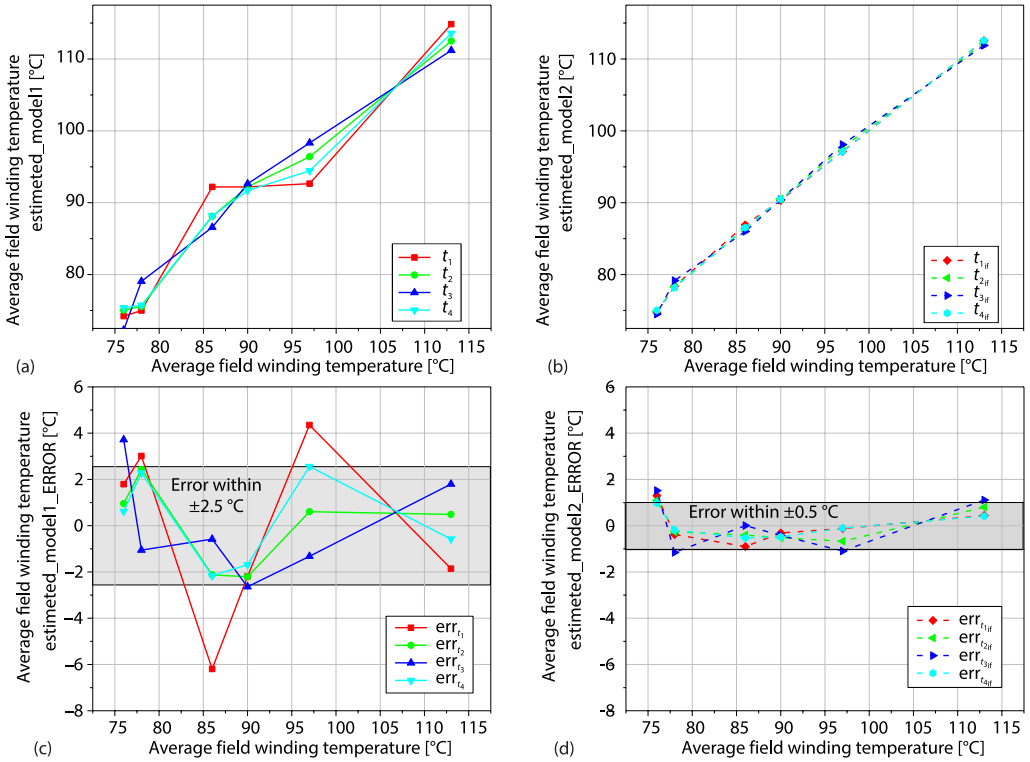

Figure 7. (a) Estimated *vs.* measured average field winding temperature using Model 1, (b) estimated *vs.* measured average field winding temperature using Model 2, (c) error calculated as the difference between estimated and measured average field winding temperature using Model 1, and (d) error calculated as the difference between estimated and measured average field winding temperature using Model 2

where A, B, C, and D are coefficients. The eq. (12) is derived using copper resistance dependence of temperature and corresponding coefficients are determined using the least squares method as well as for the eq. (13). The results are compared within field current range of interest and the obtained temperature difference is less than 1 °C, so the made assumption will not significantly affect the results when measurement uncertainties are taken into account.

Sensitivity analysis

Simple practical sensitivity analysis is performed to developed estimation models in order to determine how different values of an independent variable affect a specific dependent variable under a given set of assumptions. For the case when HG was loaded at rated value (regime No. 3 in tab. 1) the output variable is calculated for changing the single input variable, leaving all other inputs unchanged. Since the input variables are field current and temperatures it is not convenient to use per unit system. The temperatures have been changed by 0.5 °C (equal to temperature measurement error of Pt100 class B probe at 40 °C [16], reference temperature of cold air), and the current by 1% (assumed error in field current estimation when it is not measured directly). When the estimation is performed with the indirectly measured values and with developed estimation models (Models 1 and 2) the sensitivity is shown as the difference $\Delta t_{\text{rot.avg}}$ in °C when single input is changed. The sensitivity analysis results for both proposed models are shown in tab. 3.

Table 3. Calculated sensitivity of Model 1 and Model 2

Sensor group	Sensitivity 1 of Model 1^{1*}	Sensitivity 2 of Model 1^{2*}	Sensitivity 1 of Model 2^{3*}	Sensitivity 2 of Model 2^{4*}	Sensitivity 3 of Model 2^{5*}	Sensitivity 3 of Model 2^{6*}
t1	–2.89	3.90	–3.83	–0.75	–0.50	–0.42
t2	–2.04	2.62	–3.49	–0.68	–0.50	–0.36
t3	–3.03	3.55	–3.85	–0.75	–0.50	–0.52
t4	–1.76	1.72	–3.49	–0.68	–0.50	–0.46

$1^{*}\Delta t_{\text{rot.avg}}$ for tmeasured +0.5 °C, $2^{*}\Delta t_{\text{rot.avg}}$ for tcold air +0.5 °C, $3^{*}\Delta t_{\text{rot.avg}}$ for if +5%, $4^{*}\Delta t_{\text{rot.avg}}$ for if +1%,
$5^{*}\Delta t_{\text{rot. avg}}$ for tmeasured +0.5 °C, and $6^{*}\Delta t_{\text{rot.avg}}$g for tcold air +0.5 °C

The values in the tab. 3 show that the output deviations are smaller when using a model that includes the field current (Model 2) if it can be estimated with accuracy greater than 5%, in [17] achieved field current estimation accuracy is 2%. Based on the absolute value of evaluated practical sensitivity shown in tab. 3, the best results are obtained for sensor groups t_2 and t_4. This is mainly due to the sensor location and its exposure to cold air-flow.

Conclusions

In this paper problems related to field winding temperature measurement were analysed with the purpose of enhancing field winding temperature monitoring. Two models for estimating the average field winding temperature are developed based on the available measurements (field current and cold air temperature) and built in sensors that are part of the online temperature monitoring system. The first model, which is not based on field current measurement, is particularly suitable for use with brushless generators. The models are verified by results obtained during the heat run test of real 44.5 MVA HG. Validation results show that the accuracy of the presented estimation models is satisfactory especially in the range of field current close to rated value, which is more critical from the aspect of rotor dynamic overload. A simple sensitivity analysis proves the robustness of the models. The intention is to implement

the developed model on the HG's SCADA system in order to increase the reliability of field winding temperature monitoring and improve maintenance assessment.

In the next step a detailed field winding thermal model which would calculate the temperature of each part of the field winding in a thermal steady-state will be developed. Further research may include the hot spot temperature estimation that will even more increase reliability and safety of rotor temperature monitoring and dynamic overload capabilities.

Nomenclature

A – surface, [m^2]
c – specific heat capacity of air, [Jkg^{-1}K^{-1}]
q – volumetric flow, [m^{3}s^{-1}]
t – temperature, [°C]
R – winding resistance, [Ω]

Greek symbols

λ – thermal conductivity coefficient, [Wm^{-1}K^{-1}]
ρ – air density, [kgm^3]

Subscripts

air – air
f – field
th – thermal

References

[1] ***, https://www.theengineeringknowledge.com/synchronous-generator-capability-curves/
[2] ***, IEEE Std 421.5TM, IEEE Recommended Practice for Excitation System Models for Power System Stability Studies, 2005
[3] Hudon, C., *et al*., On-Line Rotor Temperature Measurements, *Proceedings*, 2014 IEEE Electrical Insulation Conference (EIC), Philadelphia, Penn., USA, 2014, pp. 373-377
[4] Hudon, C., *et al.*, Rotor Temperature Monitoring using Fiber Bragg Gratings, *Proceedings*, 2016 IEEE Electrical Insulation Conference (EIS), Montreal, Qc., Canada, 2016, pp. 456-459
[5] Mori, M., *et al*., Application of IR Thermography as a Measuring Method to Study Heat Transfer on Rotating Surface, *Forschung im Ingenieurwesen*, *72* (2008), 1, pp. 1-10
[6] Pelle, J., Souad, H., Heat Transfer Study in A Rotor-Stator System Air-Gap with an Axial Inflow, *Applied Thermal Engineering*, *29* (2009), 8-9, pp. 1532-1543
[7] Kral, C., *et al*., Rotor Temperature Estimation of Squirrel-Cage Induction Motors by Means of a Combined Scheme of Parameter Estimation and A Thermal Equivalent Model, *IEEE Transactions on Industry Applications*, *40* (2004), 4, pp. 1049-1057
[8] Stipetic, S., *et al.*, Measurement of Excitation Winding Temperature on Synchronous Generator in Rotation Using Infrared Thermography, *IEEE Transactions on Industrial Electronics*, *59* (2011), 5, pp. 2288-2298
[9] Kovačić, M., *et al*., Bluetooth Wireless Communication and 1-Wire Digital Temperature Sensors in Synchronous Machine Rotor Temperature Measurement, *Proceedings*, 14th International Power Electronics and Motion Control Conference EPE-PEMC, Ohrid, Republic of North Macedonia, 2010, pp. T7-25
[10] ***, IEEE Std 115, IEEE Guide: Test procedures for Synchronous Machines, 1995, (R2002)
[11] ***, IEEE Std 67, IEEE Guide for Operation and Maintenance of Turbine Generators, 2005
[12] Hanić, Z., *et al*., Some Problems Related Tt Surface Temperature Measurement of Synchronous Generator Excitation Winding in Rotation, *Proceedings*, 14th International Power Electronics and Motion Control Conference EPE-PEMC 2010, IEEE, Ohrid, Republic of North Macedonia, 2010, pp. T7-15
[13] ***, IEEE Std 1129, IEEE Recommended Practice for Monitoring and Instrumentation of turbine Generators, 1992
[14] Ding, H., *et al*., Estimation of Rotor Temperature of Permanent Magnet Synchronous Motor Based on Model Reference Fuzzy Adaptive Control, *Mathematical Problems in Engineering*, *2020* (2020), ID4183706
[15] Nikbakhsh, A., *et al*., Classification and Comparison of Rotor Temperature Estimation Methods of Squirrel Cage Induction Motors, *Measurement*, *145* (2019), Oct., pp. 779-802
[16] ***, IEC 60751, Industrial Platinum Resistance Thermometers And Platinum Temperature Sensors, 2008
[17] Tang, J., *et al*., Estimation Algorithm for Current and Temperature of Field Winding in Electrically Ex-Cited Synchronous Machines with High-Frequency Brushless Exciters, *IEEE Transactions on Power Electronics*, *36* (2020), 3, pp. 3512-3523

Paper submitted: December 12, 2022
Paper revised: January 30, 2023
Paper accepted: February 7, 2023